2022 IEEE/RSJ International Conference on Intelligent Robots and Systems (IROS)
October 23-27, 2022, Kyoto, Japan

Design and Evaluation of the infant Cardiac Robotic Surgical System (iCROSS)

Po-Chih Chen, Pei-An Hsieh, Jing-Yuan Huang, Shu-Chien Huang, and Cheng-Wei Chen

Abstract— **In this study, the infant Cardiac Robotic Surgical System (iCROSS) is developed to assist a surgeon in performing the patent ductus arteriosus (PDA) closure and other infant cardiac surgeries. The iCROSS is a dual-arm robot allowing two surgical instruments to collaborate in a narrow space while keeping a sufficiently large workspace. Compared with the existing surgical robotic systems, the iCROSS meets the specific requirements of infant cardiac surgeries. Its feasibility has been validated through several teleoperated tasks performed in the experiment. In particular, the iCROSS is able to perform surgical ligation successfully within one minute.**

I. Introduction

With the advantages of high precision and small incision, the success of robot-assisted surgery has been repeatedly demonstrated in laparoscopy [1], urology [2], and orthopedic surgeries [3]. However, the volume and footprint of the existing robotic surgical systems may restrict their applications to adults. For example, most patent ductus arteriosus (PDA) closure surgeries for infants are still performed manually by surgeons. The PDA is referred to the failure of the ductus arteriosus to close after birth. Such failure may cause significant mortality and potential complications, including heart failure and renal dysfunction [4]. The PDA accounts for 5% to 10% of all congenital heart diseases for newborns [5]. The prevalence of PDA is estimated to be between 20% and 50% for premature infants. The incidence grows up to 60% in those less than 29-week gestation [6], [7].

While therapeutic catheterization is becoming the treatment for young children with PDA, surgical ligation is still necessary for premature infants [4]. Robot-assisted PDA closure is confirmed feasible with the da Vinci Robotic System for children aged from 3 to 18 years [8]. The surgical maneuver is reported intuitive and precise. However, the procedure cannot be applied to infants due to the size limitation imposed by the da Vinci Robotic System. A surgical system specifically designed for infants is desirable.

In addition to the da Vinci Robotic System, there are many other commercially available robotic surgical systems. For example, the ROSA Surgical System is developed for performing minimally invasive procedures for the brain and spine [9]. However, dual-arm collaboration is an essential requirement for infant cardiac surgeries, including the PDA closure [10]. Many existing robotic systems are designed with only a single manipulator and cannot be applied here. Although it is always possible to set up two manipulators in the operating room, the surgical instruments held by the robotic manipulators, respectively, cannot be placed closely in a narrow surgical field due to the interference between the manipulators [11].

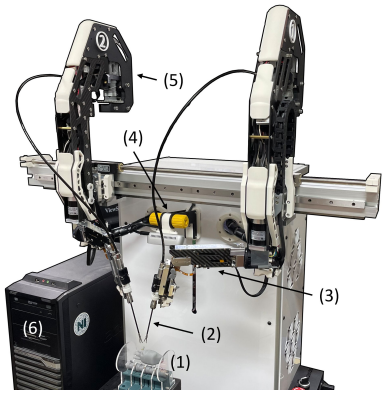

Fig. 1. The infant Cardiac Robotic Surgical System (iCROSS). (1) The infant heart model. (2) Two instruments operating simultaneously. (3) The 6-DoF robot manipulator. (4) Camera installed for teleoperation. (5) The tool driver for specific instruments applied in the infant cardiac surgery, including but not limited to forceps and clip appliers. (6) The NI LabVIEW Real-Time Target.

With a smaller and compact manipulator design, the Raven II surgical robot [12] has demonstrated its ability to delicately perform bimanual surgical tasks, such as suturing [13] and debridement [14]. However, the Raven II is not yet suitable for assisting infant cardiac surgeries, typically having only one open incision of about 15 mm. The instrument of the Raven II was designed with a diameter of 10 mm. It is very challenging to miniaturize the instrument as it contains the cable-driven mechanism that drives three degrees of freedom (DoFs) at the tooltip. Moreover, the Raven II was designed with the remote center of motion (RCM) mechanism to minimize the incision size. Collisions between the manipulators may happen when placing the RCM of each manipulator closely [15]. Some surgical robots developed explicitly for intraocular surgeries do allow two RCMs closer than 10 mm [16], [17]. However, their workspace is too small for the PDA closure surgery, for which at least a $20 \times 20 \times 60$ mm^3 volume is required.

The iCROSS, a novel robotic system aiming at remote and fully automated infant cardiac surgeries, is developed in this study. The specifications for performing infant cardiac surgeries are analyzed. The mechanical design is proceeded based

This work was supported in part by the Ministry of Science and Technology in Taiwan (Young Scholar Fellowship MOST 110-2636-E-002-006).
Corresponding author: Cheng-Wei Chen cwchenee@ntu.edu.tw
Po-Chih Chen, Pei-An Hsieh, Jing-Yuan Huang, and Cheng-Wei Chen are with the Department of Electrical Engineering, National Taiwan University, Taipei, Taiwan. Shu-Chien Huang is with the Department of Surgery, National Taiwan University Hospital, Taipei, Taiwan.

2022 IEEE/RSJ International Conference on Intelligent Robots and Systems (IROS) | 978-1-6654-7927-1/22/$31.00 ©2022 IEEE | DOI: 10.1109/IROS47612.2022.9981503

on the derived specifications. With the proposed mechanism, the dual-arm robotic system can operate two instruments in extremely close proximity without collisions. The robot also possesses enough dexterity and a sufficiently large workspace. In the end, several surgical tasks are performed to demonstrate the feasibility of the iCROSS in performing infant PDA closure.

II. Specification for PDA Closure Surgery

This study focuses on developing a robotic surgical system for assisting infant PDA closure. Causes, symptoms, and treatments for PDA are introduced in this section. In addition, the surgical procedure for PDA closure surgery is explained, along with corresponding requirements for the surgical system.

When the baby is in the womb, blood does not need to flow through the lungs because all oxygen comes from the mother. As a normal part of the circulatory system, the ductus arteriosus is the channel between the aorta and the pulmonary artery to divert the blood from the lungs to the body, as illustrated in Fig. 2. The ductus arteriosus typically closes automatically after birth. The PDA refers to the consistent opening of ductus arteriosus after birth, which affects normal blood flow and may cause morbidity and even mortality.

The PDA causes heart murmurs and thus can be diagnosed through a stethoscope by the doctor. Treatments for the PDA depend on the patient. Watchful waiting and medications are applied in some mold cases. A catheter procedure is also available for young children and adults [18]. However, an immediate surgical closure is necessary for severe cases like newborn infants.

In the PDA closure surgery, the patient is placed in a right lateral decubitus position for a better approach and visualization of the surgical field. A 15 mm incision cut between the ribs is made before the thoracotomy is performed with rib spreaders. Part of the left lung is retracted anteromedially with an angled hook to force out space for the surgery.

After making the incision, a tissue dissection is required to access the PDA, which is around 60 mm beneath the incision port. The tissue dissection around PDA was performed with electrosurgical cautery and forceps with careful attention to the vagus and recurrent laryngeal nerves. In this procedure, the iCROSS needs to adapt forceps to grasp the tissue on one manipulator, and an electrosurgical unit (ESU) dissects on the other. High precision and dexterity are required to dissect without damaging the surrounding vessels and tissues.

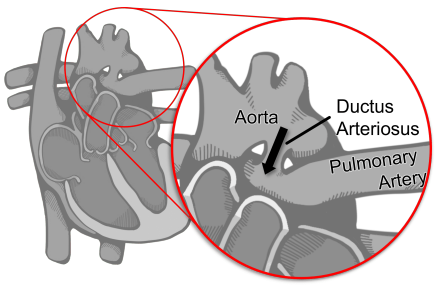

Fig. 2. A PDA is a heart defect in which the ductus arteriosus (typically with a diameter of 3 mm) does not close after birth. This defect causes blood to divert from the aorta to the pulmonary artery. Surgical ligation may be required for some cases.

After the PDA is dissected and exposed, ligation is performed. Standard methods for PDA ligation include vascular clips and stitches. With vascular clips, an endoscopic clip applier is required to place one or two vascular clips to fasten the PDA. Alternatively, two forceps are required to tie up the ductus with stitches. While vascular clips are more straightforward and less time-consuming to be applied, the stitches method is still considered a standard method with less morbidity if performed well. The actual approach may be subject to the patient's availability and the surgeon's preferences. Thus, the iCROSS must be designed to adapt both the clip applier and forceps.

After the PDA is ligated, proper suturing of tissues and skin is required. This procedure also employs two forceps simultaneously. Considering the 15 mm incision cut and 60 mm deep access, the workspace of the iCROSS is required larger than $20\times20\times60$ mm^3. In addition, the two instruments shall be able to work simultaneously inside this narrow surgical field. Therefore, when their tips are nearly aligned together, the minimum angle between the two instruments must be less than 15°. In summary, the iCROSS is designed to:

1) work with two instruments simultaneously;
2) possess 6 DoFs for each instrument and enough dexterity;
3) adapt several types of tools, including forceps, ESU, and clip applier;
4) accommodate two instruments in close proximity with an angle of intersection less than 15°;
5) possess sufficiently large workspace to cover the required surgical field, i.e., $20 \times 20 \times 60$ mm^3.

III. Mechanical Design

The iCROSS is designed for both automated and master-slave operations. The two slave manipulators are identical. Each manipulator possesses six joints and an additional DoF for driving surgical instruments. The detailed mechanical design is introduced in this section, followed by the corresponding kinematics, workspace analysis, and proximity validation of the design.

A. Slave Manipulators

The mechanical design of the iCROSS manipulators is illustrated in Fig. 3. The two joints near the base are prismatic, while the other four are revolute. Such configuration capacitates the two instruments to get extremely close during operations. In addition, the two prismatic joints reduce the number of revolute joints when maintaining sufficient DoFs, which improves the overall system accuracy.

Joints 1 and 2 are prismatic. The former is actuated by a linear motor (Linmot P02-23Sx80F-HP); two additional linear rails are deployed to support the load. The latter, on the other hand, is actuated with a ball screw driven by a DC

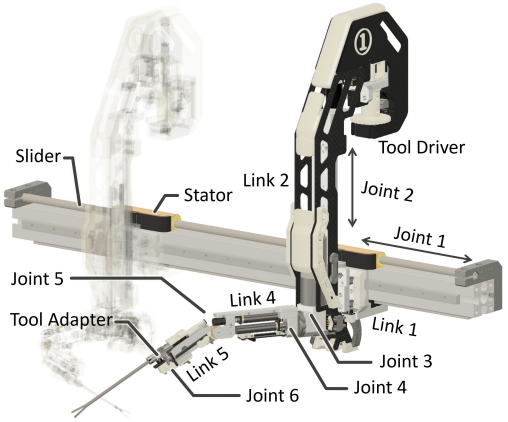

Fig. 3. The iCROSS consists of two manipulators. Each manipulator has 6 DoFs, including two prismatic joints (Joints 1 and 2) and four revolute joints (Joints 3–6). In particular, Joint 1 is actuated by a linear motor that creates a rapid response of translational movement. Joint 1 of both manipulators is coaxial as the two stators move along the same slider.

servo motor (Maxon RE 25; MR Type-ML encoder). Joint 3 is positioned at the bottom of Link 2, with A Harmonic Drive (RH-11D-3001-E100AL) utilized. Joint 4 is driven by a brushed DC servo motor (Maxon RE 13; GP13-A 275:1 planetary gearhead; MR Type-S encoder).

The key to close proximity is the miniature design of Joint 5 and Link 5. This section is part of the end-effector, and its size determines how close the two instruments can get.

To minimize the size of Joint 5, a customized worm gear mechanism is utilized, as shown in Fig. 4. On two sides of the worm gear, a bearing and a thrust ball bearing are deployed to constrain the joint; an integrated coupling shaft transmits the torque from a brushed DC servo motor (Maxon RE 13; GP13-A 17:1 planetary gearhead; MR Type-S encoder). In this design, the width of this link is only 16 mm, which allows close proximity of the two instruments. For better precision, on the other hand, a tension spring connects Links 4 and 5, compensating for the backlash of the worm gear.

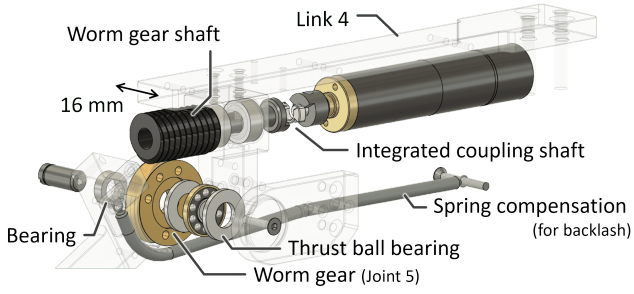

Fig. 4. Joint 5, a worm-gear-driven mechanism. This design reduces the size of the end-effector to only 16 mm, allowing the two instruments to get very close during operation. A tension spring compensates for the backlash of the worm gear.

Link 5 includes a tool housing mechanism that accommodates the tool adapter, as shown in Fig. 5. The tool adapter has two bearings to enable rotational movement when attached to the adapter housing. A spring collect mechanism (ER8 system) on the end of the tool adapter can accommodate a variety of tools with diameters less than 5mm. A spur gear is fixed on the tool adapter. A DC servo motor (Maxon RE 13; GP13-A 26:1 planetary gearhead; MR Type-S encoder) with a spur gear attached to the output shaft drives Joint 6 through the gear on the tool adapter.

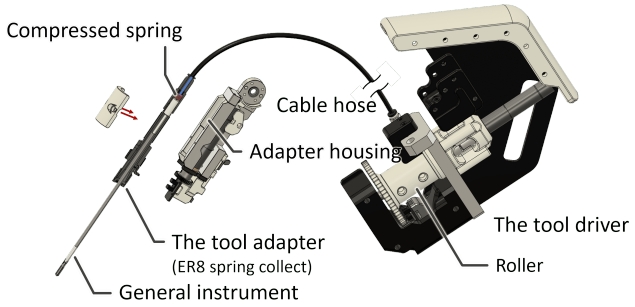

Fig. 5. Instrument adapting mechanism: the tool adapter, the adapter housing on Link 5, and the tool driver. Such a design adapts general surgical instruments and drives them through the cable-driven mechanism with a miniature end-effector, a design that allows the two instruments to get very close. Adaptable instruments include the electrosurgical unit (ESU), clip applier, and forceps.

The tool driver is designed to drive instruments like forceps and the clip applier, which requires an additional DoF for opening and closing movements. A DC servo motor (Maxon RE 13; GP13-A 275:1 planetary gearhead; MR Type-S encoder) drives the instruments with a cable roller mechanism through a cable hose, as shown in Fig.5. A compressed spring inside the tool adapter pushes against the inner shaft of the instrument, restoring its position when the cable is released.

B. Kinematics

The kinematics of the iCROSS is shown in Fig. 6. The coordinate frame of the base is assigned at the left front of the base of the iCROSS. The coordinate frame of the end-effector is assigned to have the same orientation when the

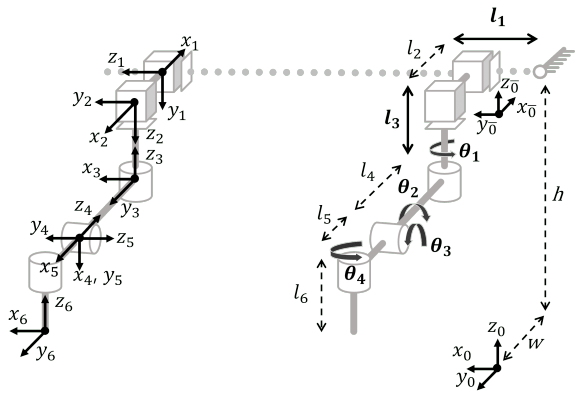

Fig. 6. Kinematic diagram of the iCROSS manipulators with the definition of coordinate frames and kinematic variables. Both manipulators share the same coordinate frames and kinematic variables. The manipulator on the right shows the position and orientation at $\theta_1 = \theta_2 = \theta_3 = \theta_4 = 0°$.

values of all joints are 0 degrees. Both arms of the iCROSS share exactly the same coordinate system, with different initial l_1 value to avoid collisions.

TABLE I

D-H PARAMETERS FOR THE KINEMATIC CHAIN

$link_i$	a_{i-1}	α_{i-1}	d_i	θ_i
$\bar{0}$	0	$0°$	h	$-90°$
1	w	$-90°$	l_1	$0°$
2	$-l_2$	$-90°$	0	$180°$
3	0	$180°$	$-l_3$	$\theta_1 - 90°$
4	0	$90°$	$-l_4$	$\theta_2 - 90°$
5	0	$90°$	0	$\theta_3 - 90°$
6	l_5	$90°$	$-l_6$	$\theta_4 - 90°$

The Denavit–Hartenberg parameters are shown in Table I. The dummy frame method [19] is applied to appropriately derive the forward kinematics, with which an augmented dummy frame $\bar{0}$ is assigned. The Jacobian technique [20] is applied to solve the inverse kinematics in real-time during operation.

TABLE II

DESIGN PARAMETERS OF THE ICROSS

Parameter	w	h	l_2	l_4	l_5	l_6
length (mm)	179.5	520	91.5	155	24.5	200

On the other hand, the design parameters of the actual system are listed in Table II. In particular, l_1 and l_3 are variables for the prismatic joints–Joints 1 and 2–and their motion ranges from 0 to 350 mm and 0 to 150 mm, respectively.

C. Workspace Analysis

The workspace and dexterity of the iCROSS are analyzed to ensure that it is sufficient for infant cardiac surgeries. This study adopts the dexterity indices developed by Wu [21] and Badescu [22], indices based on the dexterous solid angle proposed by Abdel-Malek [23]. The dexterity of a manipulator describes the possible configurations when it reaches a spatial position. The dexterity D for the spatial position p is defined as:

$$D(p) = \frac{A_R(p)}{A_S} \in (0, 1], \tag{1}$$

where A_S denotes the area of the Service Sphere, which is a unit sphere centering at this position. In addition, $A_R(p)$ denotes the area of the Service Region, which refers to all the areas on the Service Sphere that the tooltip can orientate. The discretization method is applied in this analysis. The resolution for the position is 10 mm.

The results are shown in Fig. 7, where positions with dexterity larger than 0.17 are displayed. Dexterity 0.17 accounts for $\frac{1}{6}$ area of the Service Sphere. Such dexterity is enough to perform flexible operations, which meets the design requirement of infant cardiac surgeries. In addition, the workspace is larger than a 200 × 150 × 100 mm^3 box, which is sufficient for infant cardiac surgery.

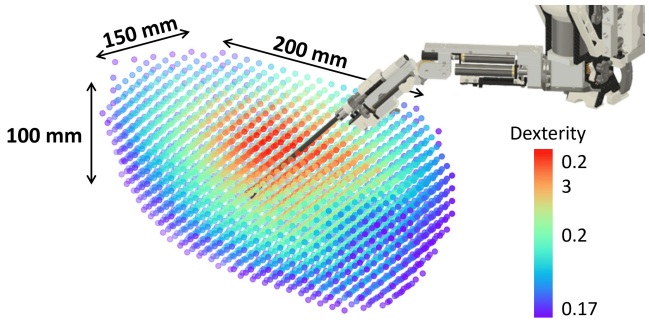

Fig. 7. The workspace of the iCROSS manipulator with the dexterity larger than 0.17.

D. Proximity Validation

The two manipulators of the iCROSS need to be able to collaborate in a narrow surgical field. As shown in Fig. 8 (a), the two instruments can get as close as 10 degrees, which meets the 15 degrees requirement. On the other hand, the two manipulators are not limited to the left and right configurations–they can also apply back and forth configurations interchangeably, as shown in Figs. 8 (b) and 8 (c). This feature allows greater flexibility when operating in a small incision.

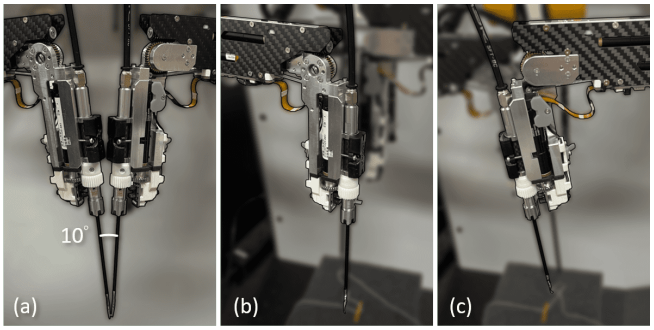

Fig. 8. Configurations of dual-arm operation using the iCROSS: (a) Two instruments work collaboratively with a minimum angle of 10 degrees. (b) The right arm is placed in front of the left arm. (c) The left arm is placed in front of the right arm.

IV. MECHATRONIC AND SOFTWARE DESIGN

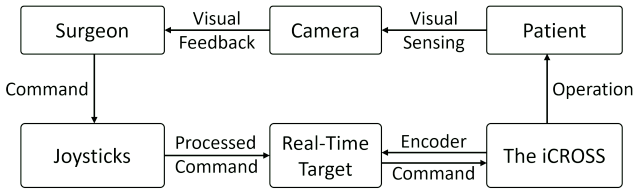

Fig. 9. The iCROSS system architecture for teleoperated surgical tasks. The surgeon commands the robotic manipulators via joysticks while receiving visual feedback from the monitor. After proper transformation, the master commands are sent to the real-time target, which calculates the inverse kinematics and drives the motors.

The system architecture is shown in Fig. 9. An NI LabVIEW Real-Time Target (Intel Core i7-3770 Processor with an NI PCIe-7841R Reconfigurable I/O Device) receives position references, calculates inverse kinematics, and controls the motors with a PID controller.

The linear motor controller (LinMot Servo Drive C1100) is connected to the Real-Time Target via the EtherCAT; the Real-Time Target controls the servo motors through customized electronics. The iCROSS performs a homing procedure at startup to ensure repeatability.

The surgeon commands the robotic manipulators via two joysticks (3D System Touch) after receiving the visual feedback on a monitor from a camera (Intel RealSense D435i). The joysticks read the spatial position, orientation, and button signals to command the corresponding manipulators. The joysticks are placed side by side with an angle θ, with which the workspace of the joysticks overlaps appropriately. The readings from the joysticks go through some post-processing, including coordinate mapping, motion scaling, and collision avoidance, before being sent to the iCROSS.

A. Coordinate Mapping

The control console setup is shown in Fig. 10. Readings from the two joysticks are transformed into a common base coordinate O_B according to their configuration. Such transformations provide a more intuitive dual-arm operation.

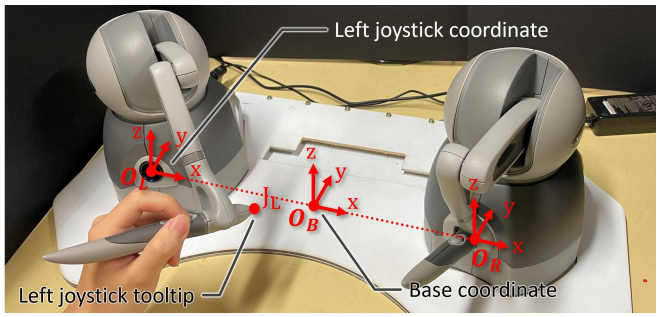

Fig. 10. Definition of coordinate frames of the master joysticks. O_L and O_R indicate the coordinates of the left and right joystick, respectively. The common coordinate, O_B, is located in the middle between O_L and O_R.

B. Collision Avoidance

To avoid collisions between the two manipulators, we implemented the Rapid Collision Detection Algorithm proposed by Yue Shen [24]. The links of the manipulators are bounded with cuboids, cylinders, and spheres as the constraints. The minimum distance between any two geometries is calculated when a collision is possible. Different approaches are adopted in different collision scenarios, e.g., cuboid and cuboid; cylinder and cylinder; cuboid and cylinders. The algorithm is precise and efficient, meeting our real-time collision avoidance requirements.

V. Experimental Results

After the whole system is integrated, corresponding evaluations are necessary. To evaluate the performance of the iCROSS and its feasibility in robot-assisted PDA closure surgery, two tasks are performed: the staple removing task and the single surgical knot-tying task. The same user teleoperates the two tasks ten times, controlling the system with the joysticks and receiving visual feedback only from the monitor.

A. Staple Removing Task

A teleoperated staple removing task is performed to evaluate the precision and flexibility of the iCROSS. Eight staples are inserted in a foam sponge sheet with different orientations: four vertical and four horizontal. The user operates the right manipulator to remove the staples and collect them into the target field, as shown in Fig. 11. The small size of the staples–0.5 mm wide and 8.4 mm long–requires a precise operation, while the different orientations challenge its dexterity.

In the task, we record the time consumption, moving distance of the tooltip, and the number of drops and dropouts. When a drop happens, the user needs to retrieve the staple. When a staple drops out of the view or cannot be picked up, it is categorized as a dropout. The results are shown in Table III: this task takes an average of 62.77 seconds; two drops and one dropout occur in the ten trials. These results indicate that iCROSS is precise and efficient enough for such a dedicated task.

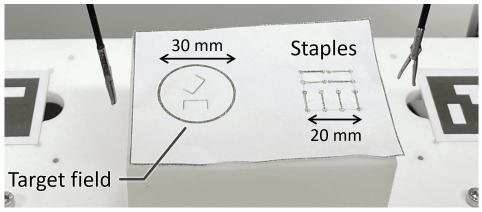

Fig. 11. Experimental setup of the staple removing task. (a) The staples are inserted into the foam sponge sheet with various orientations. The operator is asked to remove the staples in the listed order. (b) The screenshot of the real-time video stream viewed by the operator.

B. Single Surgical Knot-Tying Task

Ligation with surgical knot-tying is one of the most challenging procedures in PDA closure surgery, in which two forceps collaborate within a narrow surgical field. The surgical knot-tying task is conducted to evaluate the performance of the iCROSS in this procedure. The tying target for this task is a flexible tube with the ends attached to a foam sponge sheet. The tube is 2 mm in diameter and simulates the ductus; a 0.5 mm suture is used in this task.

The user is asked to perform a single surgical knot on the tube with the suture, as shown in Fig. 12. During the procedure, the time consumption, moving distance of tooltips, collisions between the instruments, and drops of the suture are recorded. The results are shown in Table III. On average, the task takes 70.70 seconds; a total of four suture drops and one collision occur within the ten trials. The results indicate that the iCROSS can efficiently perform complex and dexterous tasks.

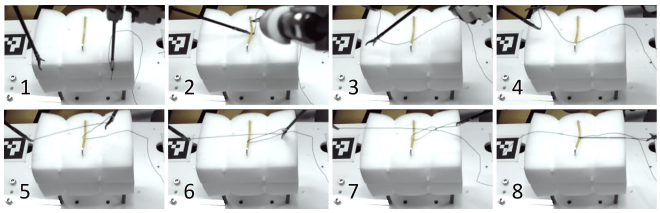

Fig. 12. Progress of surgical ligation task captured from the real-time video stream viewed by the operator: (1) pick up the suture; (2), (3) pass the suture from beneath the tube; (4), (5) circle the suture; (6) pick up the suture through the circle; (7), (8) pull and tension the suture to form a knot.

TABLE III

EXPERIMENTAL RESULTS OF THE PERFORMANCE VALIDATION. (N=10)

Tasks and parameters	Mean	SD
"Staple Removal Task"		
Time to complete (sec)	62.77	7.79
Economy of motion [Right] (cm)	176.83	12.99
Drops (n)	2	
Dropouts (n)	1	
"Single Surgical Knot-Tying Task"		
Time to complete (sec)	70.70	19.04
Economy of motion [Left] (cm)	89.10	24.70
Economy of motion [Right] (cm)	118.57	49.78
Collisions (n)	1	
Drops (n)	4	

*Values with unit n indicate the total occurrences during the N trials

VI. CONCLUSIONS AND FUTURE WORK

This study develops a novel robotic surgical system, the iCROSS, to assist in infant cardiac surgeries. The surgical requirements for infant PDA closure, which is a surgical procedure necessary for many premature infants, are analyzed and addressed in our mechanism design. The iCROSS can install and drive several surgical instruments, collaborate with two instruments simultaneously and closely, and reach a sufficiently large workspace required for infant cardiac surgeries. Experimental results have demonstrated the feasibility and performance of the iCROSS in achieving teleoperated surgical tasks, including staple removal and ligation. The robotic system will be integrated with haptic feedback and holographical display in the future. We will also conduct dry-lab experiments using the integrated surgical system.

REFERENCES

[1] A. Ng and P. Tam, "Current status of robot-assisted surgery," *Hong Kong Med J*, vol. 20, no. 3, pp. 241–250, 2014.

[2] D. R. Yates, C. Vaessen, and M. Roupret, "From leonardo to da vinci: the history of robot-assisted surgery in urology," *BJU international*, vol. 108, no. 11, pp. 1708–1713, 2011.

[3] A. Adili, "Robot-assisted orthopedic surgery," in *Seminars in laparoscopic surgery*, vol. 11, no. 2. Sage Publications Sage CA: Thousand Oaks, CA, 2004, pp. 89–98.

[4] J. E. Dice and J. Bhatia, "Patent ductus arteriosus: an overview," *The Journal of Pediatric Pharmacology and Therapeutics*, vol. 12, no. 3, pp. 138–146, 2007.

[5] D. J. Schneider and J. W. Moore, "Patent ductus arteriosus," *Circulation*, vol. 114, no. 17, pp. 1873–1882, 2006. [Online]. Available: https://doi.org/10.1161/CIRCULATIONAHA.105.592063

[6] A. Sellmer, J. V. Bjerre, M. R. Schmidt, P. J. McNamara, V. E. Hjortdal, B. Høst, B. H. Bech, and T. B. Henriksen, "Morbidity and mortality in preterm neonates with patent ductus arteriosus on day 3," *Archives of Disease in Childhood-Fetal and Neonatal Edition*, vol. 98, no. 6, pp. F505–F510, 2013.

[7] S. E. Hamrick and G. Hansmann, "Patent ductus arteriosus of the preterm infant," *Pediatrics*, vol. 125, no. 5, pp. 1020–1030, 2010.

[8] Y. Suematsu, B. N. Mora, T. Mihaljevic, and P. J. del Nido, "Totally endoscopic robotic-assisted repair of patent ductus arteriosus and vascular ring in children," *The Annals of Thoracic Surgery*, vol. 80, no. 6, pp. 2309–2313, 2005. [Online]. Available: https://www.sciencedirect.com/science/article/pii/S0003497505009744

[9] C. Batailler, D. Hannouche, F. Benazzo, and S. Parratte, "Concepts and techniques of a new robotically assisted technique for total knee arthroplasty: the rosa knee system," *Archives of Orthopaedic and Trauma Surgery*, vol. 141, no. 12, pp. 2049–2058, 2021.

[10] E. Le Bret, S. Papadatos, T. Folliguet, D. Carbognani, J. Pétrie, Y. Aggoun, A. Batisse, J. Bachet, and F. Laborde, "Interruption of patent ductus arteriosus in children: Robotically assisted versus videothoracoscopic surgery," *The Journal of Thoracic and Cardiovascular Surgery*, vol. 123, no. 5, pp. 973–976, 2002. [Online]. Available: https://www.sciencedirect.com/science/article/pii/S002252230267045X

[11] Z. Zhang, L. Zheng, Z. Chen, L. Kong, and H. R. Karimi, "Mutual-collision-avoidance scheme synthesized by neural networks for dual redundant robot manipulators executing cooperative tasks," *IEEE Transactions on Neural Networks and Learning Systems*, vol. 32, no. 3, pp. 1052–1066, 2021.

[12] B. Hannaford, J. Rosen, D. W. Friedman, H. King, P. Roan, L. Cheng, D. Glozman, J. Ma, S. N. Kosari, and L. White, "Raven-ii: an open platform for surgical robotics research," *IEEE Transactions on Biomedical Engineering*, vol. 60, no. 4, pp. 954–959, 2012.

[13] S. Aghajani Pedram, P. Ferguson, J. Ma, E. Dutson, and J. Rosen, "Autonomous suturing via surgical robot: An algorithm for optimal selection of needle diameter, shape, and path," 05 2017, pp. 2391–2398.

[14] B. Kehoe, G. Kahn, J. Mahler, J. Kim, A. Lee, A. Lee, K. Nakagawa, S. Patil, W. D. Boyd, P. Abbeel, and K. Goldberg, "Autonomous multilateral debridement with the raven surgical robot," in *2014 IEEE International Conference on Robotics and Automation (ICRA)*, 2014, pp. 1432–1439.

[15] J. Rosen, M. Lum, M. Sinanan, and B. Hannaford, "Raven: Developing a surgical robot from a concept to a transatlantic teleoperation experiment," in *Surgical Robotics*. Springer, 2011, pp. 159–197.

[16] J. T. Wilson, M. J. Gerber, S. W. Prince, C.-W. Chen, S. D. Schwartz, J.-P. Hubschman, and T.-C. Tsao, "Intraocular robotic interventional surgical system (iriss): Mechanical design, evaluation, and master–slave manipulation," *The International Journal of Medical Robotics and Computer Assisted Surgery*, vol. 14, no. 1, p. e1842, 2018.

[17] D.-D. Zhang, J. Chen, W. Li, D. Bautista-Salinas, and G.-Z. Yang, "A microsurgical robot research platform for robot-assisted microsurgery research and training," *International Journal of Computer Assisted Radiology and Surgery*, vol. 15, 10 2019.

[18] K. Wang, X. Pan, Q. Tang, and Y. Pang, "Catheterization therapy vs surgical closure in pediatric patients with patent ductus arteriosus: a meta-analysis," *Clinical Cardiology*, vol. 37, no. 3, pp. 188–194, 2014.

[19] A. Singh, A. Singla, and S. Soni, "D-h parameters augmented with dummy frames for serial manipulators containing spatial links," vol. 2014, 08 2014.

[20] F. Lewis, C. Abdallah, and D. Dawson, "Control of robot," *Manipulators, Editorial Maxwell McMillan, Canada*, pp. 25–36, 1993.

[21] L. Wu, R. Crawford, and J. Roberts, "Dexterity analysis of three 6-dof continuum robots combining concentric tube mechanisms and cable driven mechanisms," *IEEE Robotics and Automation Letters*, vol. 2, pp. 1–1, 04 2017.

[22] M. Badescu and C. Mavroidis, "New performance indices and workspace analysis of reconfigurable hyper-redundant robotic arms," *The International Journal of Robotics Research*, vol. 23, no. 6, pp. 643–659, 2004.

[23] K. A. Abdel-Malek and B. Paul, "The dexterous solid angle of robotic manipulators with a spherical wrist," in *International Design Engineering Technical Conferences and Computers and Information in Engineering Conference*, vol. 12860. American Society of Mechanical Engineers, 1994, pp. 341–350.

[24] Y. Shen, Q. Jia, G. Chen, Y. Wang, and H. Sun, "Study of rapid collision detection algorithm for manipulator," in *2015 IEEE 10th Conference on Industrial Electronics and Applications (ICIEA)*, 2015, pp. 934–938.